한국박용기관학회지 제28권, 제6호, pp. 981~992, 2004. 9 (ISSN 1226-9549)
Journal of the Korean Society of Marine Engineers

# 고정격자계에서 유한체적법을 이용한 진공동결건조 과정의 열 및 물질전달에 대한 연구

송 치 성†

(원고접수일 : 2004년 4월 21일, 심사완료일 : 2004년 6월 21일)

# A Fixed Grid Finite Volume Analysis of Multi-Dimensional Freeze Drying Process under Vacuum Condition

Chi-Sung Song†

**Abstract** : Freeze drying under vacuum condition is a complex process that involves simultaneous heat and mass transfer, sublimation of ice, and motion of sublimation front. Proper treatment of the motion of sublimation interface is crucial for an accurate prediction of the freeze drying process. Based on the enthalpy formulation that has been successfully used in liquid/solid phase change problems, a fixed grid method, streamlined for the freeze drying analysis, was developed in this study. The accuracy of the fixed grid method was checked by solving a one-dimensional tray freeze drying and a two-dimensional vial freeze drying problem and then comparing the results with those by the moving grid method. Finally, the freeze drying characteristics of two-dimensional slab and axis-symmetric cylinder was investigated using the fixed grid method.

**Key words** : Fixed Grid Method(고정격자계), Finite Vloume Method(유한체적법), Numerical Method(수치해석), Freeze Drying(동결 건조)

## Nomenclature

$C_{01}$ : Darcy flow permeability (m$^2$)

$C_1$ : constant for Knudsen flow permeability (m)

$C_2$ : ratio of effective diffusivity in porous medium to binary diffusivity

$C_p$ : heat capacity (J/kg)

$C_{sw}$ : bound water content (kg water /kg dried product)

$D_{w,in}$ : binary diffusivity of water vapor and inert gas mixture (m$^2$/s)

$D^0_{w,in}$ : $D_{w,in}P$ (N/s)

$F$ : view factor for radiation flux calculation

$f_{eq}(T)$ : equilibrium vapor pressure over

---

† 책임저자(한국기계연구원), E-mail : scs1675@kimm.re.kr, T : 042)868-7372

ice (N/m$^2$)

$f_i$ : volume fraction of ice

$k$ : thermal conductivity (W/m K)

$k_1$ : bulk diffusivity for water vapor (m$^2$/s)

$k_1 = C_2 D^0_{w,in} K_w / (C_2 D^0_{w,in} + K_{mx} P)$

$k_2, k_4$ : self diffusivity (m$^4$/Ns)

$k_2 = k_4 = k_w k_{in} / (C_2 D^0_{w,in} + K_{mx} P) + (C_{01} / \mu_{mx})$

$k_3$ : bulk diffusivity for inert gas (m$^2$/s)

$k_3 = C_2 D^0_{w,in} K_{in} / (C_2 D^0_{w,in} + K_{mx} P)$

$k_d$ : desorption rate of bound water (1/s)

$K_w$ : Knudsen diffusivity (m$^2$/s)

$K_w = C_1 (R_g T / M_w)^{0.5}$

$K_{in}$ : Knudsen diffusivity (m$^2$/s)

$K_{in} = C_1 (R_g T / M_{in})^{0.5}$

$K_{mx}$ : mixture Knudsen diffusivity for binary gas (m$^2$/s)

$K_{mx} = y_w K_{in} + y_{in} K_w$

$L$ : thickness of drying material (m)

$M$ : molecular weight (kg/mol)

**N** : mass flux of gas (kg/m$^2$s)

$P$ : total pressure in dried region, or pressure (N/m2)

$q$ : heat flux (W/m$^2$)

$R_g$ : universal gas constant (J/molK)

$R$ : radius or length of drying material (m)

$T$ : temperature (K)

$t$ : time (s)

$r, x, z$ : Coordinate (m)

$y$ : mole fraction

Greek Letters

$\varepsilon$ : porosity

$\triangle h_s$ : heat of sublimation of ice (J/kg)

$\triangle h_v$ : heat of vaporization of bound water (J/kg)

$\mu$ : viscosity (kg/ms)

$\rho$ : density (kg/m$^3$)

$\sigma$ : Stefan-Boltzmann constant (W/m$^2$K$^4$)

Superscript

0 : initial value

Subscript

0 : freeze drying chamber

$I$ : dried region

$II$ : frozen region

$e$ : effective value

$f$ : film heat transfer

$g$ : gas

$HP$ : heating plate

$in$ : inert gas

$w$ : water vapor

## 1. Introduction

Freeze drying is a process that directly dehydrates products using the sublimation of ice at frozen state. As the freeze drying is performed at sub-zero temperatures and vacuum pressures, freeze dried products are almost free from thermal and chemical degradation. Therefore, the freeze drying is considered as a most proper drying technique for heat-sensitive and high-value products such as quality foods, pharmaceuticals, bio-products [1-3].

Freeze drying is a typical moving boundary problem that accompanies the motion of sublimation interface which separates the domain into a dried and a frozen region. There exist two solution strategies for the moving boundary problems according to the used grid system. Those are a moving grid method and a fixed grid method. In the moving grid method, the position of interface is explicitly tracked and different governing equations for the different regions are solved (two domain method). However, in the fixed grid method, a new variable that measures the phase composition is introduced and a single set of governing equations is solved for all domain (single domain method). The effect of the motion of interface is included by changing cell properties or adding source terms according to the phase composition. Then the position of the interface can be only implicitly obtained using the calculated distribution of the phase composition. In case of the freeze drying problem, an ice fraction $f_i$ that denotes volume content of ice is a proper variable that represents the phase composition.

Analytical solutions for sublimation problems in porous media have been published by many researchers [4-6]. However, the prediction of the industrial freeze drying processes requires numerical methods due to the complex geometry and operation conditions. Most of numerical studies on the freeze drying were based on the sorption-sublimation model [7-10]. Also there are other analyses based on simpler models [11-14]. As numerical schemes, moving grid methods based on the finite element method [15,16] and the finite difference method [1,7,8,9,10] were mainly used. The finite volume method based on the fixed grid method was used to solve a one-dimensional microwave freeze drying of food stuffs [13,14].

In this study, a two-dimensional finite volume calculation program with a fixed grid system was developed. The multi-dimensional sorption-sublimation model [10] was used to describe the dynamic behavior in the primary and secondary drying stage. Skim milk solution was selected as a model of drying material.

## 2. Calculation Model

Schematic diagram of the freeze drying during the primary drying stage is shown in Fig. 1. In the primary drying stage, the drying chamber is depressurized with a vacuum pump and a cold trap and the temperature of the heating plate is simultaneously increased to provide the heat of sublimation. In the fig. 1 the drying material is divided into a dried region and a frozen region by a sublimation interface. Water vapor is produced by the sublimation of ice at the interface and it diffuses through the pores to exit the drying material. As the freeze drying continues the frozen region decreases in size with the motion of the sublimation interface. Once all the ice in the drying material is removed, the temperature of the heating plate is increased again to a higher temperature to allow desorption of bound water in the dried region, which is secondary drying stage.

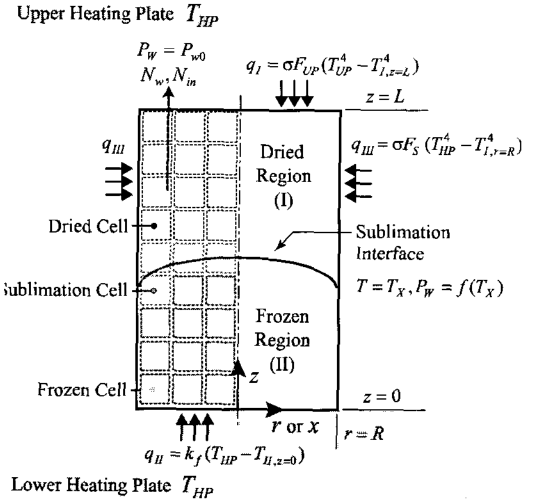

**Fig. 1 A schematic diagram of freeze drying in the primary drying stage**

The quantities $q_{\mathrm{I}}$, $q_{\mathrm{II}}$ and $q_{\mathrm{III}}$ shown in Fig. 1 represent the heat fluxes at the top, bottom and side wall of the drying material. For example, in the freeze drying in a vial, the heat transferred through the side wall is considerable. That heat flux causes a curved isotherm and a spatially non-uniform sublimation. The configuration of the sublimation interface is distorted due to these multi-dimensional heat transfer effects in the vial freeze drying. The parameter $\boldsymbol{N}_w$ represents the mass flux of water vapor and $\boldsymbol{N}_{in}$ represents the mass flux of inert gas. However, the mass flux of inert gas can be neglected in most cases, because the amount of inert gas is small compared to the amount of water vapor present in the drying chamber. In Fig. 1, each volume cell is categorized into dried, frozen and sublimation cells according to its ice fraction.

## 3. Mathematical Formulation

In the fixed grid method, only one energy equation is sufficient for the heat transfer calculation. That is

$$\rho C_p \frac{\partial T}{\partial t} + \nabla \cdot ( \mathbf{N}_w C_{pg} - k \nabla T) = \Delta h_v \rho_l \frac{\partial C_{sw}}{\partial t} + \Delta h_s(\rho_{II} - \rho_l) \frac{\partial f_i}{\partial t} \tag{1}$$

The energy equation, Eq. (1), is similar to a standard energy equation with conduction and convection heat transfer except for the last two terms which represent latent heat sources due to the vaporization of bound water and the sublimation of ice. The heat capacity and thermal conductivity in Eq. (1) are functions of ice fraction $f_i$, written as

$$\rho C_p = f_i \rho_{II} C_{pII} + (1 - f_i) \rho_{Ie} C_{pIe} \tag{2}$$

$$k = f_i k_{II} + (1 - f_i) k_{Ie} \tag{3}$$

For dried cells ($f_i = 0$) and for frozen cells ($f_i = 1$), the heat capacity and thermal conductivity reduce to those of the dried region and those of the frozen region. For sublimation cells ($0 < f_i < 1$), they are determined to be average values weighted by the ice fraction.

The governing equation for the vaporization of the bound water is a simple rate equation, written as

$$\frac{\partial C_{sw}}{\partial t} = - k_d (1 - f_i) C_{sw} \tag{4}$$

where $k_d$ is a desorption rate constant [9]. By inserting $(1 - f_i)$ in Eq. (4), the desorption of bound water in the frozen cells are suppressed in the fixed grid method.

The governing equation for the temporal change of the ice fraction $f_i$ in the sublimation cells is

$$(\rho_{\text{II}}-\rho_{\text{I}})\frac{\partial f_i}{\partial t}=-\nabla\cdot\boldsymbol{N}_w \quad (5a)$$

Eq. (5a) states that vapor generation (divergence of vapor flux) in each sublimation cell is equal to reduction of ice content in the cell. By integrating Eq. (5a) over a cell volume $\Delta V$, Eq. (5a) can be rewritten as

$$(\rho_{\text{II}}-\rho_{\text{I}})\triangle V\frac{\partial f_i}{\partial t}=-\sum_{j=e,w,n,s}\boldsymbol{N}_w\cdot\boldsymbol{A}_j \quad (5b)$$

Here, $\mathbf{A}_j$'s are outward normal vectors of the control surfaces that comprise the sublimation cell. As the temporal change of the ice fraction is localized at the sublimation cells, the latent heat source term due to sublimation is 0 in dried and frozen cells. For frozen cells, the vapor mass flux $\boldsymbol{N}_w$ is 0, and thus the governing energy equation for the frozen cells reduces to a conduction equation.

Heat flux conditions at the surfaces are

$$q_{\text{I}}=\sigma F_{UP}(T_{HP}^4-T_{z=L}^4) \quad (6)$$

$$q_{\text{II}}=k_f(T_{HP}-T_{z=0}) \quad (7)$$

$$q_{\text{III}}=\sigma F_s(T_{HP}^4-T_{r=R}^4) \quad (8)$$

where $F$ is a radiation shape factor, $k_f$ is the film thermal conductivity, and $T_{HP}$ is the temperature of the heating plate. A symmetry condition is imposed at the boundary of $r=0$ or $x=0$.

The governing equations for mass transfer in the dried region are

$$\varepsilon\frac{M_w}{R_g}\frac{\partial}{\partial t}\left(\frac{P_w}{T}\right)+\nabla\cdot\mathbf{N}_w=-\rho_{\text{I}}\frac{\partial C_{sw}}{\partial t} \quad (9)$$

$$\varepsilon\frac{M_{in}}{R_g}\frac{\partial}{\partial t}\left(\frac{P_{in}}{T}\right)+\nabla\cdot\mathbf{N}_{in}=0 \quad (10)$$

Eq. (9) and Eq. (10) are derived from the conservation for water vapor and inert gas in the dried region. The last term in Eq. (9) is the mass source due to the vaporization of bound water, shown in Eq. (4). In the fixed grid method, the above equations are solved only in the dried cells. The mass flux is always 0 in the frozen cells, and thus no pressure exists there. In the sublimation cells, the local thermodynamic equilibrium can be assumed. Thus, at the sublimation cells, the vapor pressure is equal to an equilibrium vapor pressure of the temperature at that cell.

$P_w=f_{eq}(T)$, for all sublimation cells. (11)

Therefore, the sublimation cells act like boundaries for the pressure calculation.

To complete Eq. (9) and Eq. (10), we need constitute equations for vapor flux $\boldsymbol{N}_w$ and inert gas flux $\boldsymbol{N}_{in}$. The consititutive equations derived from the dusty-gas model [1,17] are

$$\boldsymbol{N}_w=-\frac{M_w}{R_gT}[k_1\nabla P_w+k_2P_w(\nabla P_w+\nabla P_{in})] \quad (12)$$

$$\boldsymbol{N}_{in}=-\frac{M_{in}}{R_gT}[k_3\nabla P_{in}+k_4P_{in}(\nabla P_w+\nabla P_{in})] \quad (13)$$

where the dusty-gas model takes Knudsen diffusion, bulk diffusion, and the convective flow into full account. With Eq. (12) and Eq. (13), the governing equations for partial pressures are completed. In the present analysis, the calculation on the inert gas was omitted as inclusion of inert gas calculation produced practically no differences in the results.

Boundary conditions for the mass transfer are

$$P_w = P_{w0}, P_{in} = P_{in0}, \text{ for open surfaces,} \quad (14)$$

$$\boldsymbol{N}_w = \boldsymbol{N}_{in} = 0, \text{ for walls.} \quad (15)$$

The pressures at open surfaces of the drying material are defined to be same as the pressures in the drying chamber. For walls, the mass flux is zero.

In addition to above, all variables are assumed to be uniform at the beginning of the simulation at except the ice fraction is initially 1, such as

$$T = T^0, P_w = P^0_w, P_{in} = P^0_{in}, C_{sw} = C_{sw}, f_i = 1 \quad (16)$$

## 4. Numerical Procedure

Overall numerical procedure is shown in Fig. 2. First, the volume cells were defined to be the dried, the frozen, and the sublimation cells according to their ice fraction. Then the temperatures were obtained for whole domain by solving the energy conservation equations. The vapour pressures and bound water concentration in the dried and sublimation cells were then calculated. When all the variables were tentatively determined, the ice fraction in each sublimation cell was updated from the mass conservation. The calculation of temperature, pressure, bound water concentration and ice fraction was repeated until all the variables converge to a given level of accuracy in the $10^7$ range. Finally, the calculation for next time step was started by updating the time and variables.

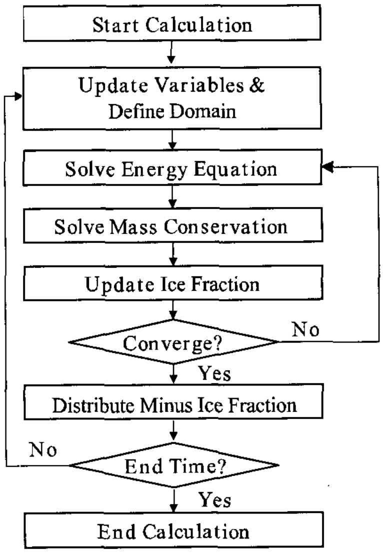

**Fig. 2 Flowchart for overall numerical procedure of the present analysis**

For spatial and temporal discretizations, a second order central difference and a first order implicit method were used. The time step was automatically adjusted for the ice fraction not to change more than 0.01, and maximum time step was set to 12 sec. The resulting algebraic equations for temperature and vapour pressure were solved using a bi-conjugate gradient solver. A successive substitution with under-relaxation was used as an iterative method to handle the coupling of the heat and mass transfer, the sublimation of ice, and the motion of the sublimation front.

## 5. One-Dimensional Tray Freeze Drying

To check the accuracy of the present fixed grid calculation, an one-dimensional tray freeze drying problem reported by Liapis and Bruttini [8] was solved using both moving grid and fixed grid methods.

The finite volume analysis program with a moving grid method has been developed by the authors [18]. The properties and operation conditions for the simulation are presented in Table 1. The moving grid calculation was done with 20 grid points, 10 in each dried and frozen region. For the fixed grid calculation, 40 equally spaced grid points were used.

**Table 1 Parameter value and expressions for analysis of the freeze drying of skim milk in a tray[8].**

| | |
|---|---|
| $C_{01}$ | $7.219\times10^{-15}$ ($m^2$) |
| $C_1$ | $3.85583\times10^{-4}$ (m) |
| $C_2$ | 0.921 |
| $C_{pg}$ | 1616.6 (J/kg·K) |
| $C_{ple}$ | 2590.0 (J/kg·K) |
| $C_{pll}$ | 1930.0 (J/kg·K) |
| $C^0_{sw}$ | 0.6415 |
| $D^0_{w,in}$ | $0.00014931(T^3(1/M_w+1/M_{in}))^{0.5}$ ($kg\cdot m/s^3$) |
| $k_d$ | $6.48\times10^{-7}(s^{-1})$ for primary drying<br>$7.8\times10^{-5}(s^{-1})$ for secondary drying |
| $k_{le}$ | $1.412\times10^{-3}\ P+0.2165$ (W/m·K) |
| $k_{ll}$ | $488.19/T+0.4685$ (W/m·K) |
| $k_f$ | $1.5358P$ (W/m·K) |
| $L$ | 0.02 (m) |
| $P^0_{in}, P_{in0}$ | 4.00 (Pa) |
| $P^0_w, P_{w0}$ | 1.07 (Pa) |
| $T^0$ | 233.15 (K) |
| $T_{HP}$ | 313.15 (K) |
| $f_{eq}(T)$ | $133.3224\ \mathrm{Exp}(-2445.5646/T + 8.23121\ \log_{10}(T)\ \ 0.0167T + 1.20514\times10^{-5}T^2\ \ 6.757169)$ (Pa) |
| $\triangle h_s$ | 2840000 (J/kg) |
| $\triangle h_v$ | 2687400 (J/kg) |
| $\varepsilon$ | 0.785 |
| $\mu_{mx}$ | $18.4858[T^{1.5}/(T+650)]$ (kg/m·s) |
| $\rho_l$ | 328.0 ($kg/m^3$) |
| $\rho_{le}$ | 215.0 ($kg/m^3$) |
| $\rho_{ll}$ | 1030.0 ($kg/m^3$) |

In Fig. 3, the results by the fixed grid method and those of the moving grid method [18] are plotted together. Fig. 3 clearly shows that the accuracy of the fixed grid method is comparable to that of the moving grid method, which is contradicts the general belief that the moving grid method is indispensable for accurate prediction of freeze drying processes. Considering that only 40 grid points were used for this fixed grid calculation, the results are very satisfactory.

The nature of the fixed grid calculation can be observed by the temperature history shown in Fig. 3(b). Small jumps in the sublimation temperature history calculated by the fixed grid method (dashed line) are due to the change in domain (e.g., a frozen cell becomes a sublimation cell and then a dried cell, subsequently) with time. But such small jumps are not observed in the drying rate curved in Fig. 3(a).

## 6. Two Dimensional Vial Freeze Drying

A vial freeze drying problem reported by Sheehan and Liapis [10] has been solved to check the accuracy of the fixed grid method in the multi-dimensional freeze drying analysis. The properties and operation conditions are same as those of the tray freeze drying simulation (Table 1) except presented in Table 2. The side wall of a vial does not allow mass transfer (impermeable) but it allows the heat transfer by radiation. The moving grid calculation was done with 200 grid points, 1010 in each dried and frozen region. For the fixed grid calculation, 1040 equally spaced grid points were used.

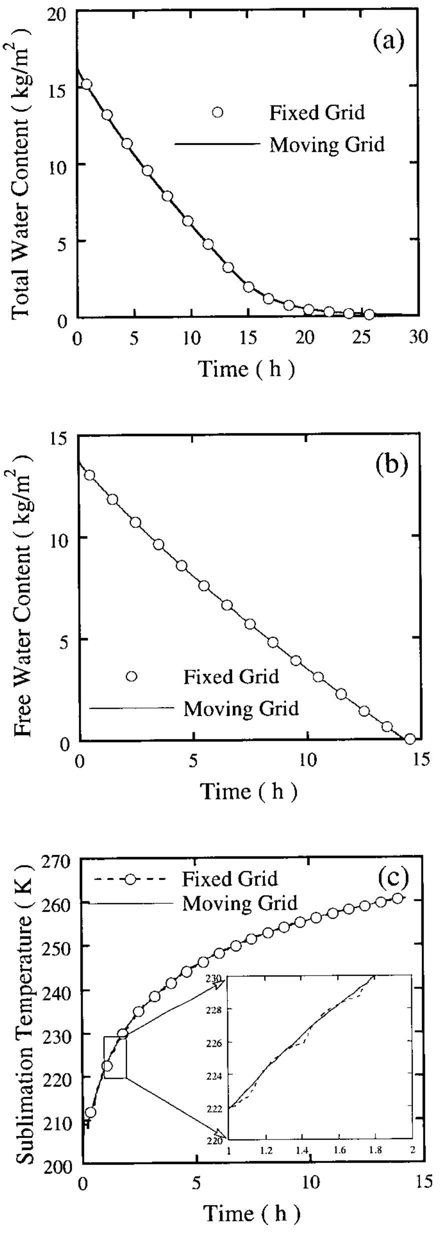

Fig. 3 Comparison of fixed grid and moving grid results for one-dimensional freeze drying in a tray: (a) total water content, (b) free water content, and (c) sublimation temperature

Table 2 Complementary boundary conditions for analysis of the freeze drying of skim milk in a vial [10].

| | |
|---|---|
| $R$ | 0.005 (m) |
| $k_f$ | 29.13 (W/m·K) |
| $F_s$ | 0.75 |
| $F_{UP}$ | 0.795 |
| $T_{HP}$ | 273 K (primary), 313 K (secondary) |

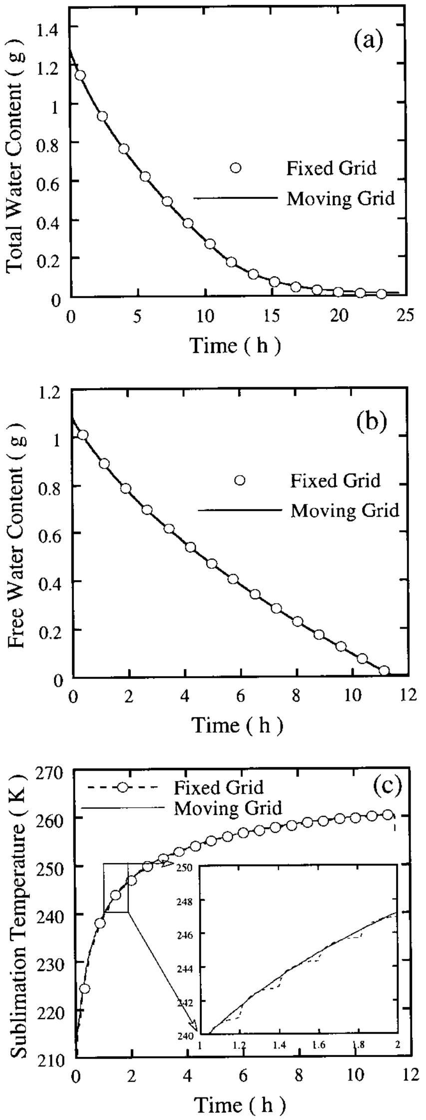

Fig. 4 Comparison of fixed grid and moving grid results for two-dimensional freeze drying in a vial: (a) total water content, (b) free water content, and (c) sublimation temperature

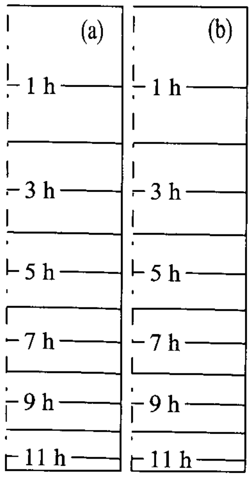

**Fig. 5 Comparison of sublimation interface position calculated by (a) fixed grid and (b) moving grid method**

In Fig. 4, the results obtained by the fixed grid method and the moving grid method are plotted for comparison. The fixed grid method is again sufficiently accurate for prediction of the multi-dimensional freeze drying in a vial. The positions of the sublimation interface at the interval of 1 hour are shown in Fig. 5. In the vial freeze drying, the curvature of sublimation interface is not very large in most cases. In Fig. 6, the heat flux through each surface of a vial during the primary drying stage is plotted. It is clearly shown that the heat transfer through the side wall is comparable to that through the bottom surface (surface area of side wall is 8 times larger than that of bottom surface).

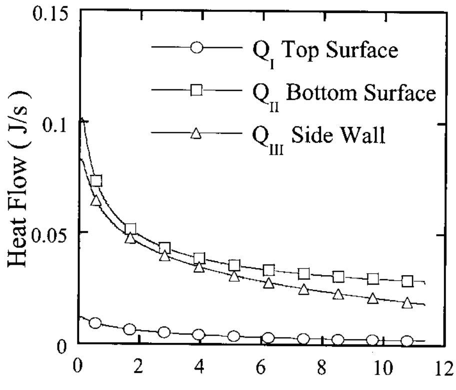

**Fig. 6 Heat flow through the top, bottom, and side surfaces of a vial**

## 7. Two-Dimensional FreezeDrying of Slab and Cylinder Objects

Finally, the freeze drying problems of two-dimensional slab and cylinder object are simulated to demonstrate the versatility of the fixed grid method over moving grid method. Now, the side surface of the drying material is assumed to be permeable and thus to allow the mass transfer. In this case, sublimation interface moves inward from the top and side surfaces. Different from the vial freeze drying, now the sublimation interface is much curved. One example of that process is the freeze drying of meat patty.

For the calculation, the same properties and operation conditions for the vial freeze drying simulation was used except the vapor pressure in the drying chamber $P_{w0}$ is 100 Pa. Another difference is the dimension of the drying material, that is, the thickness $L$ and the radius $R$ (or length in slab simulation) is set to 0.01 m. The equally spaced 2020 fixed grid points were used.

In Fig. 7, the sublimation interface positions for the freeze drying of slab and cylinder objects are plotted with respect to time. It is well shown that the sublimation interface moves from the surfaces open to ambient (top and right side) toward inner core. The free water removal ratio and the sublimation temperature history are shown in Fig. 8. Each sublimation temperature increases rather constantly with time. Compared with the sublimation temperature histories for the tray or vial freeze drying simulation, shown in Fig 3(b) and Fig. 4(b), the trend is reversed. This is partially due to the vapor pressure in the drying chamber for the freeze drying of slab and cylinder objects is much higher than the other simulations.

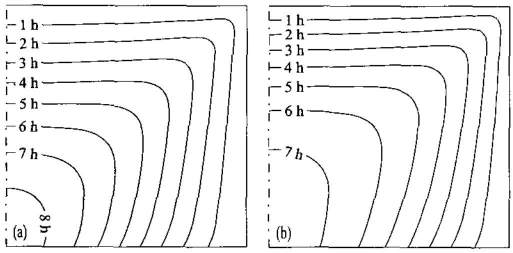

**Fig. 7 Sublimation interface position calculated by fixed grid method: (a) slab and (b) cylinder objects**

## 8. Conclusion

In this study, a finite volume calculation procedure based on a fixed grid method has been developed. The multi-dimensional sorption-sublimation model was used as a freeze drying model to accurately model the sublimation of ice (primary drying) and desorption of bound water (secondary drying). The one-dimensional tray freeze drying and two-dimensional, axis-symmetric vial freeze drying were simulated using the fixed grid calculation program developed. Comparison between the results of the fixed grid method and moving grid method has demonstrated the accuracy of the fixed grid method. Using the analysis program, two-dimensional freeze drying processes of slab and cylinder objects were simulated to demonstrate the versatility of the fixed grid method.

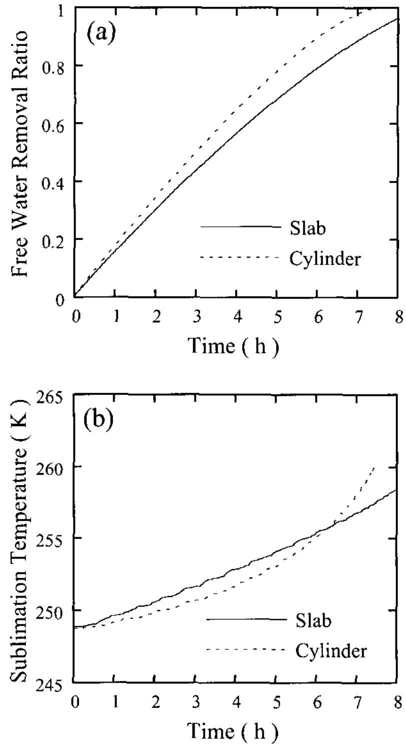

**Fig. 8 (a) Free water removal ratio and (b) sublimation interface temperature of slab and cylinder objects**

## References

[1] Millman, M.J., Liapis, A.I. and Marchello, J.M., 1985, An Analysis of the Lyophilization Process using a Sorption-Sublimation Model and Various Operation Policies, *AIChE Journal* 31, 1594-1604

[2] Liapis, A.I., 1987, Freeze Drying, pp. 295-326, in A.S. Mujumdar (Ed.) *Handbook of Industrial Drying*, Marcel Dekker, Inc., New York.

[3] Ratti, C., 2001, Hot Air and Freeze-Drying of High-Value Foods: a Review, *Journal of Food Engineering* 49, 311-319.

[4] Lin, S., 1981, An Exact Solution of the Sublimation Problem in a Porous Medium, Journal of Heat Transfer 103, 165-168.

[5] Fey, Y.C. and Boles, M.A., 1988, Analytic Study of Vacuum-Sublimation in an initially partially filled Frozen Porous Medium with Recondensation, *International Journal of Heat and Mass Transfer* 31, 1645-1653.

[6] Peng, S.-W. and Chen, G.-Q., 1994, Coupled Heat and Mass Transfer with One Discrete Sublimation Moving Interface and One Desorption Mushy Zone, *Journal of Heat Transfer* 116, 215-220.

[7] Liapis, A.I. and Litchfield, R.J., 1979, Optimal Control of a Freeze Dryer, *Chemical Engineering Science* 34, 975-981.

[8] Liapis, A.I. and Bruttini, R., 1994, A Theory for the Primary and Secondary Drying Stages of the Freeze-Drying of Pharmaceutical Crystalline and Amorphous Solutes: Comparison between Experimental Data and Theory, *Separations Technology* 4, 144-155.

[9] Sadikoglu, H. and Liapis, A.I., 1997, Mathematical Modeling of the Primary and Secondary Drying Stages of Bulk Solution Freeze-Drying in Trays: Parameter Estimation and Model Discrimination by Comparison of Theoretical Results with Experimental Data, *Drying Technology* 15, 791-810.

[10] Sheehan, P. and Liapis, A.I., 1998, Modeling of the Primary and Secondary Drying Stages of the Freeze Drying of Pharmaceutical Products in Vials: Numerical Results obtained from the Solution of a Dynamic and Spatially Multi-Dimensional Lyophilization Model for Different Operation Policies, *Biotechnology and Bioengineering* 60, 712-728.

[11] Ang, T.K., Ford, J.D. and Pei, D.C.T., 1977, Microwave Freeze-Drying of Food: A Theoretical Investigation, *International Journal of Heat and Mass Transfer* 20, 517-526.

[12] Lombrana, J.I., Elvira, C.D. and Villaran, M.C., 1997, Analysis of Operation Strategies in the Production of Special Foods in Vials by Freeze Drying, *International Journal of Food and Technology* 32, 107-115.

[13] Wang, Z.H. and Shi, M.H., 1998, Numerical Study on Sublimation-Condensation Phenomena during Microwave Freeze Drying, *Chemical Engineering Science* 53, 3189-3197.

[14] Wang, Z.H. and Shi, M.H., 1998, The Effect of Sublimation-Condensation Region on Heat and Mass Transfer during Microwave Freeze Drying, *Journal of Heat Transfer* 120,

654-660.

[15] Ferguson, W.J. and Lewis, R.W., 1993, A Finite Element Analysis of Freeze-Drying of a Coffee Sample, *Computer Methods in Applied Mechanics and Engineering* 108, 341-352.

[16] Mascarenhas, W.J., Akay, H.U. and Pikal, M.J., 1998, A Computational Model for Finite Element Analysis of the Freeze-Drying Process, *Computer Methods in Applied Mechanics and Engineering* 148, 105-124.

[17] Evans, R.B., Watson, G.M. and Mason, E.A., 1962, Gaseous Diffusion in Porous Media, *Journal of Chemical Physics* 36, 1894-1902.

[18] Song, C.S., Nam, J.H., Kim, C.-J. and Ro, S.T., 2002, A Finite Volume Analysis of Vacuum Freeze Drying Processes of Skim Milk Solution in Trays and Vials, *Drying Technology* 20, 283-305.

## 저자소개

**송치성 (宋致成)**

1983년 한국해양대학 기관학과 졸업, 1989년 동 대학 대학원 기계과 졸업, 공학석사, 2001년 서울대학교 대학원 기계과 졸업, 공학박사, 선박기계기술사, 1989.3-현재 한국기계연구원 책임연구원.